Large Load-Controlled Multiple-Active Multiple-Passive Antenna Arrays: Transmit Beamforming and Multi-User Precoding

Konstantinos Ntougias, Dimitrios Ntaikos, Bobby Gizas, George K. Papageorgiou, Constantinos B. Papadias
Athens Information Technology (AIT), Athens, Greece.
Email: kontou, dint, bogi, gepa, cpap@ait.gr

***Abstract*—In this work, we present the design of a novel large load-controlled multiple-active multiple-passive (LC-MAMP) antenna array that operates at 19.25 GHz. In addition, we describe a method that enables us to perform robust, low-complexity, arbitrary channel-dependent precoding with such arrays as well as a communication protocol that limits the computational complexity associated with beam tracking and dynamic load computation in static or low-mobility scenarios, such as indoor wireless access or wireless terrestrial backhaul use cases. Finally, we study the application of various user- and symbol-level precoding schemes in coordinated multiple-input multiple-output setups equipped with LC-MAMP arrays and we evaluate their performance through numerical simulations using a realistic channel model. The simulation results show that LC-MAMPs outperform equivalent digital antenna arrays.**

***Index Terms*—Load-controlled multiple-active multiple-passive arrays (LC-MAMP); coordinated multi-cell multiple-input multiple-output (Co-MC-MIMO); constructive-interference zero-forcing beamforming (CI-ZFBF); centimetre-wave (cm-wave) access; terrestrial backhaul.**

I. Introduction

In view of the spectral shortage, wireless network operators have adopted recently the multi-user multiple-input multiple-output (MU-MIMO) technology, in order to accommodate the enormous mobile data traffic volume [1] through multi-user spatial multiplexing (SM). To this end, precoding-based multi-user interference (MUI) mitigation is required. Typically, simple but suboptimal, in terms of the achieved sum-rate (SR) throughput, linear precoding methods are utilized.

In [4] is described a symbol-level zero forcing beamforming (ZFBF) method. This technique leaves unaffected the symbol-level interference that leads to an increase of the receive signal-to-noise-ratio (SNR) and cancels only the destructive interference. This approach is very useful in cases where a system operates in the low SNR regime, given that typically the transmission power is constrained to an upper bound. Numerical simulation results have shown that this constructive interference ZFBF (CI-ZFBF) scheme outperforms its user-level counterpart [4].

In view of the extreme capacity requirements of 5^{th} generation (5G) networks [5], the focus of the community has been shifted lately on multi-cell MIMO (MC-MIMO) paradigms, such as coordinated MC-MIMO (Co-MC-MIMO) [6] and massive MIMO [7], which are able to further increase the spectral efficiency (SE) of the system by enabling universal frequency reuse and aggressive multi-user SM.

The SM and interference management capabilities of MU-/ MC-MIMO techniques depend in general on the number of transmit antennas. This is due to the fact that the array degrees-of-freedom (DoF) provided by conventional digital antenna systems equal the number of antenna elements. On the other hand, though, in such arrays each antenna element is connected to a radio frequency (RF) chain. Moreover, the inter-element distance should be large enough, in order to avoid the occurrence of mutual coupling among the antennas which would reduce the radiation efficiency of the array. Furthermore, as the number of antennas increases, the overhead of channel state information (CSI) feedback (which is required to perform precoding) grows accordingly. These cost, complexity, power consumption, size and communication overhead constraints limit the number of antennas in practical array implementations [2]. Therefore, there is a growing interest today on hybrid analog-digital antenna systems that are able to provide a higher number of DoF for a given number of RF modules or a target number of DoF with fewer RF units than conventional digital antenna arrays (DAA), thus leading to performance enhancement or to cost and power consumption savings, respectively.

Load-controlled multiple-active multiple-passive (LC-MAMP) arrays constitute a representative example. These antenna systems are comprised by a few active elements (i.e. antennas fed by a RF unit) surrounded by multiple passive elements deliberately placed in close vicinity to them and terminated to analog loads. The strong mutual coupling induces currents to the so-called parasitic elements. By adjusting the impedance of the parasitic loads, we can control the amplitude and phase of these currents and, thus, perform adaptive transmit BF [2]. In [8] has been described a technique than enables us to perform also channel-dependent precoding with such arrays. However, design constraints limit the universal application of this method for each precoding scheme and input signal constellation. In [9] is presented a workaround to this problem. Nevertheless, the proposed technique is not robust neither is computationally light.

Nowadays, there is a trend of moving to higher frequencies, such as centimetre-wave (cm-wave) bands, in order to exploit the available spectral resources [5]. Moreover, due to the high

ISBN 978-0-9928626-7-1

burden placed on the mobile backhaul (MBH) by the capacity requirements of contemporary and future mobile broadband services, it is studied the transition of the MU-MIMO and MC-MIMO paradigms from the wireless access domain to the wireless backhaul domain. Also, the deploymend of small-cell networks (SCN) in urban environments, which enable more aggressive frequency reuse [5], implies that often the wireless backhaul nodes are compact, low-cost, low-power small-cell base stations (BS). Under this context, it becomes apparent that the design of LC-MAMPs that operate in cm-wave frequencies is highly desirable today for both wireless access and backhaul applications. In dense setups in particular, the use of simple, low-cost arrays that generate relatively wide beams and the utilization of precoding to mitigate the interference is a promising alternative against the standard backhauling practice of using complex, high-cost, highly directive antennas. Nevertheless, we have to note that beam tracking is in general a challenging task in high frequencies, especially in high mobility scenarios. Also, we should mention that the dynamic calculation of the loading values of load-controlled parasitic antenna arrays (LC-PAA) has discouraged so far the utilization of this technology in practice.

The goal of this work is to introduce a pragmatic approach that solves the aforementioned problems and facilitates the use of the LC-PAA technology in future wireless access and MBH systems. More specifically, in this paper we present the design of a novel large LC-MAMP array that operates at the 19.25 GHz. Furthermore, we describe a robust, low-complexity, arbitrary channel-dependent precoding technique for such arrays as well as a workaround to the on-the-fly load computation and beam tracking issues which is suited mainly to low-mobility scenarios. Finally, we study various user- and symbol-level precoding schemes applied in LC-MAMP-equipped Co-MC-MIMO setups and evaluate their performance through numerical simulations based on a realistic channel model.

II. Proposed MAMP Antenna Array Design

In Fig. 1 we present our novel antenna design. It is based on a bowtie patch antenna operating at 19.25 GHz. Each bowtie element has a small gap between its two branches. In this gap either a port or a load (capacitor or inductor) is placed. For the case of the port (SMA connector) the bowtie element is considered to be active (denoted with red color in Fig. 1) and for the case of the load the element is considered to be passive (denoted with green color in Fig. 1). There are four active and forty parasitic elements in total. The MAMP array was simulated with an electromagnetic analysis simulation software that implements the finite element method (FEM). The substrate chosen for the simulation is the Rogers RO4350 which has a relative permittivity of $\epsilon_r = 3.48$ and a dielectric loss tangent of $tan\delta = 0.004$ and is widely used for planar antennas at the 20 GHz frequency regime.

In Fig. 2 we present the three main view planes of the 3D far field radiation pattern of the MAMP antenna, provided that only one antenna is active at any given time.

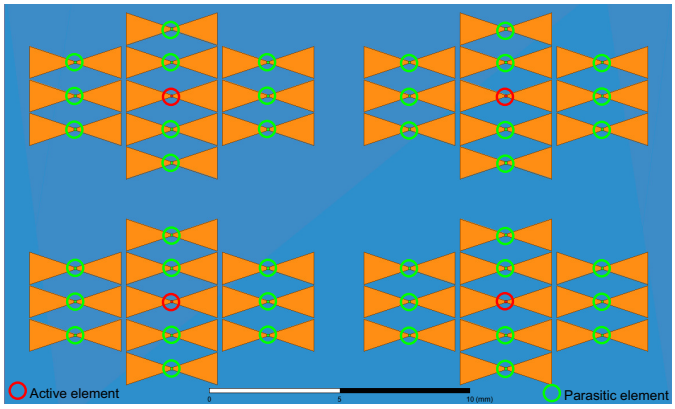

Fig. 1: MAMP antenna array with 4 active and 40 parasitic elements.

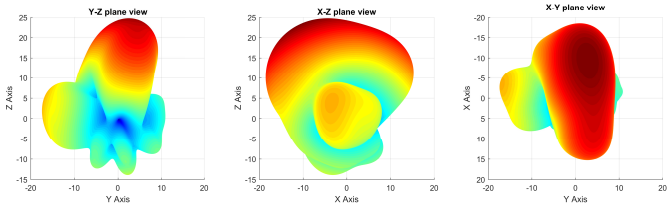

Fig. 2: 3D far field radiation patterns. The three main view planes.

III. Robust Arbitrary Precoding Technique

Consider a LC-PAA with L active antenna elements and M antennas in total. The relation between the currents and voltages associated with the antenna elements of this array is given by the generalized Ohm's law [10]:

$$\mathbf{i} = (\mathbf{Z} + \mathbf{Z}_L)^{-1} \mathbf{v}, \tag{1}$$

where $\mathbf{i}$ is the $(M \times 1)$ vector of the currents that run on the antenna elements; $\mathbf{Z}$ is the $(M \times M)$ mutual coupling matrix whose diagonal entry Z_{mm} represents the self-impedance of the mth antenna element while the off-diagonal entry Z_{mk} denotes the mutual impedance between the mth and the kth antenna element; $\mathbf{Z}_L$ is the $(M \times M)$ diagonal load matrix whose diagonal elements are the source resistances $R_1, \ldots, R_L$ and the impedances of the parasitic loads jX_m $(m = M - L + 1, \ldots, M)$, with $j = \sqrt{-1}$ denoting the imaginary unit; and $\mathbf{v}$ is the $(M \times 1)$ voltage vector that holds the L feeding voltages $v_1, \ldots, v_L$.

The system model of a $(M, (K, 1))$ MU-MIMO setup formed between a BS with M transmit antennas and K single-antenna user terminals (UT) is given from an antenna perspective by [10]

$$\mathbf{y} = \mathbf{H}\mathbf{i} + \mathbf{n}, \tag{2}$$

where $\mathbf{y}$ is the $(K \times 1)$ vector of open-circuit voltages at the receive antennas, $\mathbf{i}$ represents the $(M \times 1)$ vector of currents that run on the transmit antennas, $\mathbf{H}$ denotes the $(K \times M)$ composite channel matrix whose entry h_{km} relates the mth input current with the kth open-circuit output voltage, and $\mathbf{n}$

ISBN 978-0-9928626-7-1 © EURASIP 2017

constitutes a $(K \times 1)$ additive white Gaussian noise (AWGN) vector with covariance matrix $\mathbf{R}_n = \sigma_n^2 \mathbf{I}_K$, where σ_n^2 is the noise variance and $\mathbf{I}_K$ is the $(K \times K)$ identity matrix.

Assuming the application of channel-aware precoding, Eq. (2) becomes

$$\mathbf{y} = \mathbf{HWs} + \mathbf{n}, \tag{3}$$

where $\mathbf{W}$ is the $(M \times M)$ precoding matrix and $\mathbf{s}$ is the $(M \times 1)$ input signal vector. Hence, in order to apply channel-aware precoding to a MAMP, we have to map the precoded symbols to the antenna currents as follows [8]:

$$\mathbf{i} = \mathbf{Ws}, \tag{4}$$

and then calculate the corresponding loading values that can generate these currents. However, we should ensure that the input resistance, which depends on the loads, is positive, in order to guarantee that the antenna system will not reflect power back [11]. Since the loading values depend on the precoded signals, it becomes apparent that this design condition cannot be met for any given input signal constellation or precoding scheme. A workaround was proposed in [9]. In this work, the input signal is approximated by another one which leads to a feasible set of loading values, provided that the mean square error (MSE) of the approximation is minimum. Nevertheless, this method is computationally demanding and it is not robust.

On the other hand, it is known that LC-PAAs can admit any input signal in transmit BF applications. Based on this remark, an alternative approach that enables the performance of robust, low-complexity, arbitrary channel-aware precoding with such arrays has been described in [12]: First, transmit BF using any valid method is applied and then channel-aware precoded transmission over the employed beams takes place.

IV. Low-Complexity Communication Protocol

In low-mobility scenarios, such as dense SCN and wireless MBH setups, we can overcome the problems of beam tracking and dynamic load computation by using a number of fixed loading sets corresponding to predetermined radiation patterns (i.e. beams) and switching through these sets instead of utilizing tunable loads. In this Section, we describe a communication protocol that takes into account the aforementioned design. This protocol can be applied in both MU-MIMO and Co-MC-MIMO setups. The system operation is divided in three phases [12]:

1) **Learning phase:** For each beam combination, the BS(s) sends a pilot signal. Then, the UTs measure their signal-to-interference-plus-noise-ratio (SINR) or estimate the gain of the direct and cross channels and report back this channel quality metric.
2) **Beam-selection phase:** After switching through all possible beam combinations, the BS(s) selects the optimum one, in terms of the achieved SR throughput, based on the information reported by the UTs.
3) **Transmission phase:** The BS(s) transmits precoded signals over the selected beams.

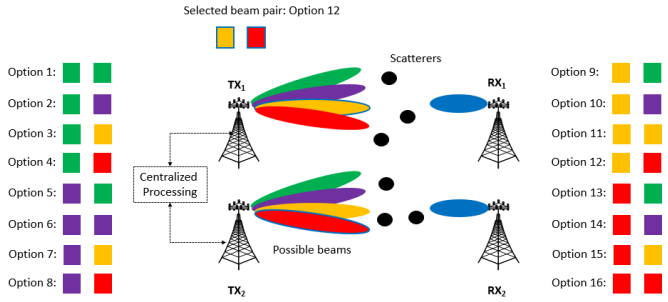

Fig. 3: A Co-MC-MIMO system comprised by 2 transmit and 2 receive nodes equipped with the LC-PAA described in Sec. II. Each transmit LC-PAA can generate at each time one out of four different beams. The best beam combination is selected jointly by the transmitters, based on SINR or CSI feedback from the receivers. Then, precoded transmission takes place over these beams.

Note that the use of SINR feedback has been included as a low-feedback alternative to the conventional CSI feedback procedure. After SINR-feedback-based beam selection, a CSI-feedback procedure for the selected composite "beam-channel" should take place, in order to enable the use of precoding. Note also that the complexity of the learning process can be reduced by using a broadcast beam and building a lookup table. This extension has been left as a future work.

V. System Model and Linear Precoding Schemes

The input-output relationship of a $(K,(K,1))$ MIMO broadcast channel (BC) formed between a BS with $M = K$ transmit antennas and K single-antenna UTs, assuming that linear precoding is utilized, is given by

$$y_k = \mathbf{h}_k^\dagger \left(\sum_{m=1}^{K} \mathbf{w}_m \sqrt{p_m} s_m \right) + n_k, \quad k = 1, 2, \ldots, K \tag{5a}$$

$$\mathbf{y} = \mathbf{HWP}^{1/2}\mathbf{s} + \mathbf{n}, \tag{5b}$$

where $\mathbf{y}$ is the $(K \times 1)$ vector of received signals y_k; $\mathbf{H}$ denotes the $(K \times K)$ channel matrix, whose rows $\mathbf{h}_k$ are $(1 \times K)$ vectors that hold the channels h_{km} between the kth user and each one of the K transmit antennas; $\mathbf{W}$ represents the $(K \times K)$ precoding matrix, whose column $\mathbf{w}_k$ is the $(K \times 1)$ BF vector for the kth user; $\mathbf{P}$ is the $(K \times K)$ power allocation matrix, whose element p_k is the power allocated to the kth user; $\mathbf{s}$ refers to the $(K \times 1)$ symbol vector, with s_k being the data symbol intended for the kth user; and $\mathbf{n}$ is the additive noise vector, whose elements n_k represent the noise at the kth receiver.

The SINR at the kth user is expressed as

$$\mathrm{SINR}_k = \frac{\left|\mathbf{h}_k^\dagger \mathbf{w}_k\right|^2 p_k}{\sum_{m \neq k} \left|\mathbf{h}_k^\dagger \mathbf{w}_m\right|^2 p_m + \sigma_n^2}, \quad k = 1, 2, \ldots, K. \tag{6}$$

ISBN 978-0-9928626-7-1 © EURASIP 2017

The data rate of the kth user is given by

$$R_k = \log_2\left(1 + \text{SINR}_k\right), \tag{7}$$

and the SR throughput is

$$R = \sum_{i=1}^{K} R_k = \sum_{i=1}^{K} \log_2\left(1 + \text{SINR}_k\right). \tag{8}$$

In ZFBF, the inner product of a user's BF vector with other users' channel vectors is zero, i.e. the MUI is nulled:

$$\left\|\mathbf{h}_k^{\dagger}\mathbf{w}_m^{(\text{ZF})}\right\|^2 = 0, \quad k, m = 1, 2, \ldots, K,\ m \neq k. \tag{9}$$

Hence, the received signal of the kth user can be expressed as

$$y_k = \mathbf{h}_k^{\dagger}\sqrt{p_k}\mathbf{w}_k^{(\text{ZF})}s_k + n_k, \quad k = 1, 2, \ldots, K. \tag{10}$$

Thus, the SINR at the kth user is given by

$$\text{SINR}_k^{(\text{ZF})} = \left\|\mathbf{h}_k^{\dagger}\mathbf{w}_k^{(\text{ZF})}\right\|^2 p_k, \quad k = 1, 2, \ldots, K. \tag{11}$$

The precoding matrix is the (column-wise normalized) Moore-Penrose pseudo-inverse of the multi-user channel matrix [12]:

$$\mathbf{F}^{(\text{ZF})} = \mathbf{H}^{+} = \mathbf{H}^{\dagger}\left(\mathbf{H}\mathbf{H}^{\dagger}\right)^{-1}. \tag{12a}$$

$$\mathbf{W}^{(\text{ZF})} = \frac{\mathbf{F}^{(\text{ZF})}(:,k)}{\|\mathbf{F}^{(\text{ZF})}(:,k)\|}, \quad k = 1, 2, \ldots, K. \tag{12b}$$

ZFBF performs well at the DoF-limited high-SNR regime but poorly at the power-limited low-SNR regime, since the BF vectors do not match the channel vectors of the intended users.

Requlatized ZFBF (RZFBF) is an extension of ZFBF where the pseudo-inverse of the composite channel matrix is regularized. The regularization coefficient is typically set such that the SINR at the users is maximized [12]:

$$\mathbf{v}_k^{(\text{RZF})} = \mathbf{H}^{\dagger}\left(\frac{1}{p_k}\mathbf{I}_K + \mathbf{H}\mathbf{H}^{\dagger}\right)^{-1}, \quad k = 1, 2, \ldots, K. \tag{13a}$$

$$\mathbf{w}_k^{(\text{RZF})} = \frac{\mathbf{v}_k^{(\text{RZF})}}{\|\mathbf{v}_k^{(\text{RZF})}\|}, \quad k = 1, 2, \ldots, K. \tag{13b}$$

RZFBF outperforms ZFBF in low and medium SNR levels and converges to ZFBF at high SNR.

In the Joint Transmission (JT) variant of Co-MC-MIMO, a "super MIMO-BC" is formed by the ensemble of transmit and receive antennas. Therefore, the system and precoding models described in this Section apply in the JT scenario as is.

VI. Constructive-Interference ZFBF

Consider a $(K, (K, 1))$ MU-MIMO system. Let us define the $(K \times K)$ channel cross-correlation matrix $\mathbf{R}$ as [4]

$$\mathbf{R} = \mathbf{H}\mathbf{H}^{\dagger}. \tag{14}$$

The symbol-to-symbol co-channel interference (CCI) from s_k to s_m is expressed as

$$\text{CCI}_{km} = s_k\rho_{km}, \quad k, m = 1, 2, \ldots, K,\ m \neq k \tag{15}$$

while the cumulative CCI on s_k from all symbols is given by

$$\text{CCI}_k = \sum_{k=1}^{K} s_k\rho_{km}, \quad m = 1, 2, \ldots, K,\ m \neq k \tag{16}$$

where

$$\rho_{km} = \frac{\mathbf{h}_k\mathbf{h}_m^{\dagger}}{\|\mathbf{h}_k\|\,\|\mathbf{h}_m\|} \tag{17}$$

is the (k, m)-th element of $\mathbf{R}$ that represents the cross-correlation factor between the kth user's channel and the mth transmitted data stream.

In CI-ZFBF, the precoding matrix has the following form [4]:

$$\mathbf{W}^{(\text{CIZF})} = \mathbf{W}^{(\text{ZF})}\mathbf{T} = \mathbf{H}^{\dagger}\mathbf{R}^{-1}\mathbf{T}. \tag{18}$$

The received signal at the kth user is given by [13]

$$y_k = \tau_{kk}\sqrt{p_k}s_k + \sum_{m \neq k} \text{CI}_{km} + n_k, \quad k, m = 1, 2, \ldots, K \tag{19}$$

where $\text{CI}_{km} = \tau_{km}\sqrt{p_m}s_m$ denotes the constructive CCI from the mth user to the kth user and τ_{km} is the (k, m) element of the $K \times K$ matrix $\mathbf{T}$. Then, the kth user's SINR is given by

$$\text{SINR}_k^{(\text{CIZF})} = \sum_{m=1}^{K} |\tau_{km}|^2 p_m, \quad k = 1, 2, \ldots, K. \tag{20}$$

$\mathbf{T}$ is calculated on a symbol-by-symbol basis as follows [4]: First, $\mathbf{R}$ is calculated according to Eq. (14). Next, assuming the use of Binary Phase Shift Keying (BPSK) modulation (i.e., $s_k = \pm 1$, $k = 1, 2, \ldots, K$), the $(K \times K)$ matrix $\mathbf{G}$ is computed as

$$\mathbf{G} = \text{diag}(\mathbf{s})\text{Re}(\mathbf{R})\text{diag}(\mathbf{s}). \tag{21}$$

Then, $\tau_{kk} = \rho_{kk}$ and $\tau_{km} = 0$ if $g_{km} < 0$ or $\tau_{km} = \rho_{km}$ otherwise. Similar relations to Eq. (21) hold for other modulation types.

Since the input signal has a finite alphabet, we use the following relationship to calculate the capacity [13]:

$$R = (1 - \text{BLER})m, \tag{22}$$

where $m = 1$ bit/symbol for BPSK and the block error rate (BLER) is given by $\text{BLER} = 1 - (1 - P_e)^{N_f}$, with P_e being the symbol / bit error rate (SER / BER) of BPSK and N_f being the frame size.

VII. Numerical Simulation Results

In this Section, we evaluate the performance of the proposed arbitrary precoding framework and communication protocol for a Co-MC-MIMO setup through numerical simulations that take into account the radiation pattern of the LC-MAMP described in Sec. II, the scattering environment and the propagation mechanisms in the 19.25 GHz band.

In Fig. 4 the average SR throughput of ZFBF JT over fixed beams in two Co-MC-MIMO systems comprised by 2 BSs serving 2 single-antenna UTs each is depicted. One system is equipped with LC-PAAs having a single active element at each time, while the other makes use of equivalent single-RF

ISBN 978-0-9928626-7-1 © EURASIP 2017

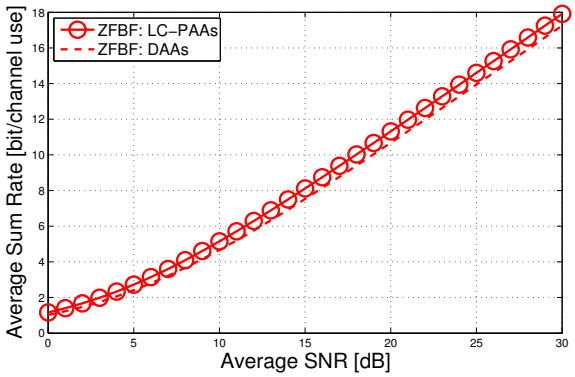

Fig. 4: SR throughput of JT ZFBF in two MC-MIMO setups equipped with LC-PAAs and DAAs, respectively.

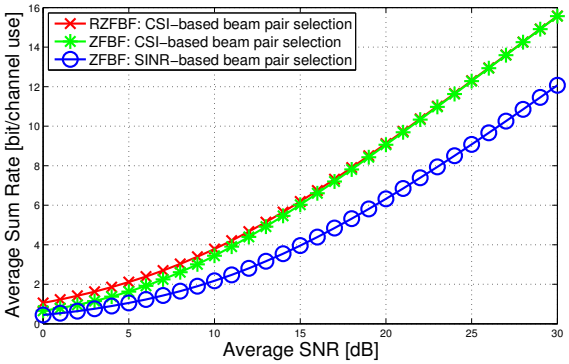

Fig. 5: Performance of the communication protocol described in Sec. IV.

DAAs. We note that the LC-MAMP setting is slightly better than the DAA one, due to the higher array gain attributed to the parasitics.

In Fig. 5 the performance of the system setup shown in Fig. 3 is depicted. The considered scenarios include beam pair selection based on SINR feedback and on CSI feedback. In the former case, the use of ZFBF is assumed, while in the latter one both ZFBF and RZFBF are considered. The employed Co-MC-MIMO variant is JT. We note that beam pair selection based on CSI feedback improves significantly the performance of ZFBF. Also, as expected, RZFBF outperforms ZFBF in low SNR values.

Finally, in Fig. 6 the performance of CI-ZFBF against ZFBF in the aforementioned setup is presented. The use of BPSK modulation is assumed. We note that CI-ZFBF performs much better than its user-level counterpart.

VIII. Conclusion

In this paper, we described the design of a novel LC-MAMP that operates at cm-wave frequencies. We presented also an approach that enables us to perform robust, low-complexity, arbitrary multi-cell precoding with such arrays as well as a low-complexity communication protocol and we

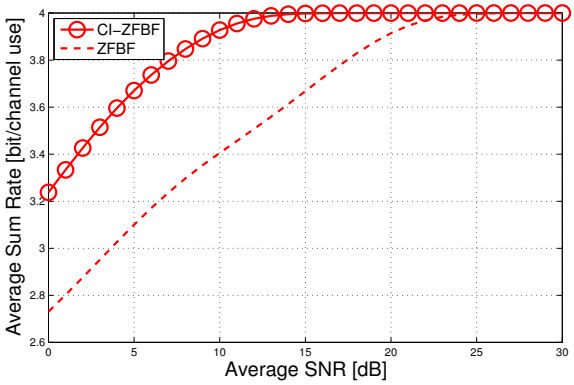

Fig. 6: SR throughput of CI-ZFBF vs. ZFBF for the same Co-MC-MIMO setup as in Fig. 5.

evaluated various user- and symbol-level precoding methods via numerical simulations. We observed that LC-MAMPs outperform equivalent DAAs.

Acknowledgement

This work has been supported by the EC H2020 Research Project SANSA (grant agreement no: 645047).

References

[1] Ericsson, "Mobility Report," Tech. Rep., June 2016.

[2] A. Kalis *et al.*, Eds., *Parasitic Antenna Arrays for Wireless MIMO Systems*. Springer-Verlag New York, 2014.

[3] H. Huang *et al.*, Eds., *MIMO Communication for Cellular Networks*. Springer-Verlag New York, 2012.

[4] C. Masouros and E. Alsusa, "Dynamic linear precoding for the exploitation of known interference in MIMO broadcast systems," *IEEE Transactions on Wireless Communications*, vol. 8, no. 3, pp. 1396–1404, March 2009.

[5] 5G-PPP, "5G Vision," Tech. Rep., February 2015.

[6] D. Lee *et al.*, "Coordinated Multipoint Transmission and Reception in LTE-Advanced: Deployment Scenarios and Operational Challenges," *IEEE Communications Magazine*, vol. 50, no. 2, pp. 148–155, February 2012.

[7] E. Larsonn *et al.*, "Massive MIMO for Next Generation Wireless Systems," *IEEE Communications Magazine*, vol. 52, no. 2, pp. 186–195, February 2014.

[8] G. Alexandropoulos *et al.*, "Precoding for multiuser mimo systems with single-fed parasitic antenna arrays," in *IEEE Global Communications Conference (GLOBECOM)*, Austin, TX, USA, December 8-12 2014, pp. 3897–3902.

[9] L. Zhou *et al.*, "Achieving arbitrary signals transmission using a single radio frequency chain," *IEEE Transactions on Communications*, vol. 63, no. 12, pp. 4865–4878, October 2015.

[10] V. Barousis *et al.*, "A new signal model for MIMO communications with compact parasitic arrays," in *IEEE International Symposium on Communications, Control and Signal Processing*, Athens, Greece, May 21-23 2014, pp. 109–113.

[11] V. Barousis and C. B. Papadias, "Arbitrary precoding with single-fed parasitic arrays: Closed-form expressions and design guidelines," *IEEE Wireless Communications Letters*, vol. 3, no. 2, pp. 229–232, February 2014.

[12] K. Ntougias *et al.*, "Coordinated MIMO with Single-fed Load-Controlled Parasitic Antenna Arrays," in *17th IEEE International Workshop on Signal Processing advances in Wireless Communications (SPAWC 2016)*, Edinburgh, UK, July 3-6 2016, pp. 1–5.

[13] ——, "Robust Low-Complexity Arbitrary User- and Symbol-Level Multi-Cell Precoding with Single-fed Load-Controlled Parasitic Antenna Arrays," in *23rd International Conference on Telecommunications (ICT 2016)*, Thessaloniki, Greece, May 16-18 2016, pp. 1–5.